Magnetoelectric coupling in the type-I multiferroic ScFeO_{3}

G. Giovannetti, D. Puggioni, P. Barone, S. Picozzi, J. M. Rondinelli, and M. Capone

Phys. Rev. B **94**, 195116 — Published 9 November 2016

DOI: 10.1103/PhysRevB.94.195116

Magneto-electric coupling in type-I multiferroic $ScFeO_3$

G. Giovannetti,[1,2,3] D. Puggioni,[4] P. Barone,[5,6] S. Picozzi,[5] J. M. Rondinelli,[4] and M. Capone[2,1]

[1] *CNR-IOM-Democritos National Simulation Centre*
[2] *International School for Advanced Studies (SISSA), Via Bonomea 265, I-34136, Trieste, Italy*
[3] *Institute for Theoretical Solid State Physics, IFW-Dresden, PF 270116, 01171 Dresden, Germany*
[4] *Department of Materials Science and Engineering, Northwestern University, Evanston, IL 60208, USA*
[5] *Consiglio Nazionale delle Ricerche (CNR-SPIN), Via Vetoio, I-67010 L'Aquila, Italy*
[6] *Graphene Labs, Istituto Italiano di Tecnologia, via Morego 30, 16163 Genova, Italy*

We investigate the electronic structure and the ferroelectric properties of the recently discovered multiferroic $ScFeO_3$ by means of ab-initio calculations. The $3d$ manifold of Fe in the half-filled configuration naturally favors an antiferromagnetic ordering, with a theoretical estimate of the antiferromagnetic Néel temperature in good agreement with the experimental values. We find that the inversion symmetry-breaking is driven by the off-centering of Sc atoms, which results in a large ferroelectric polarization of $\sim 105\,\mu C/cm^2$. Surprisingly the ferroelectric polarization is sensitive to the local magnetization of the Fe atoms resulting in a large negative magnetoelectric interaction. This behavior is unexpected in type-I multiferroic materials because the magnetic and ferroelectric orders are of different origins.

I. INTRODUCTION

Multiferroic (MF) materials display two or more ferroic orders, e.g., magnetism and ferroelectricity, often with a mutual interplay between the primary order parameters (magnetoelectric coupling) [1]. Designing these materials to have high ferroic ordering temperatures and strong responses would allow them to serve as a materials platform for many practical logic and memory applications [2].

Multiferroics can be classified according to the origin of the coexisting magnetic and ferroelectric orders [3]. In type-I multiferroics, ferroelectricity and magnetic order arise largely independent of each other, as each originates from different atomic sublattices; nonetheless, coupling between order parameters remains possible. Examples of type-I multiferroics are $BiFeO_3$ [4] and $Sr_{1-x}Ba_xMnO_3$ [5], which present high magnetic ordering temperatures and large ferroelectric polarizations. Instead in type-II MFs, magnetism induces ferroelectricity, implying a strong coupling between the two orders. Known examples of type-II multiferroics are RMn_2O_5 [6] and $RMnO_3$ [7] (R = Rare Earth). In these materials the low-temperature magnetic structure lifts inversion symmetry [8, 9] and gives rise to the ferroelectric distortion.

The distinction between the two MF classes is expected to be reflected in the strength of the magnetoelectric coupling. It should be much stronger in type-II multiferroics compared to type-I. There are, however, examples that challenge this notion. In $BiFeO_3$, a small negative magnetoelectric coupling with a variation of ferroelectric polarization ($\sim 40\,nC/cm^2$) has been observed at the onset of the magnetic ordering [10]. Also, the cycloidal modulation of its antiferromagnetic phase has been ascribed to an inhomogeneous magnetoelectric coupling, which rotates the direction of the magnetization and is uniquely determined by the ferroelectric polarization [11, 12]. A larger effect was found in $Sr_{1-x}Ba_xMnO_3$ where there is a substantial decrease in the electric polarization ($\sim 13\mu C/cm^2$) at the magnetic critical temperature [5, 13]. These findings motivate us to re-examine the established notion of the magnetoelectric coupling strength in type-I multiferroics.

Recently $ScFeO_3$ has been synthesized under 15 GPa at a temperatures above 1100 K [14] and a number of other polymorphs can be realized in thin films [15]. The high-pressure phase exhibits a polar $R3c$ space group with highly distorted ScO_6 and FeO_6 octahedra [14]. It exhibits weak ferromagnetism, of potential interest for applications [16], with an high magnetic ordering temperature of 545 K owing to a canted G-type antiferromagnetic (AFM) ordering of the Fe^{3+} atoms [14].

Multiferroic $ScFeO_3$ shares the same $R3c$ space group of $LiNbO_3$ and $BiFeO_3$ and displays a "mixture" of their electronic and ferroelectric properties. In materials with very small tolerance factor, t [17], as $ScFeO_3$ ($t = 0.83$) and $LiNbO_3$ ($t = 0.85$), the $a^-a^-a^-$ tilt pattern in Glazer notation [18] is electrostatically and energetically unstable because the A-site is severely underbonded. To stabilize the structure and optimize the environment of the A-site, a ferroelectric distortion which involves the A-cation is needed [19]. This is different from $BiFeO_3$ where the origin of the ferroelectric distortion is the stereochemical activity of the $6s^2$ lone-pair of the Bi^{3+} cation [20]. On the other hand, the B-site of $ScFeO_3$ is magnetic as in $BiFeO_3$, in contrast with the non-magnetic Nb cation in $LiNbO_3$. Note that $ScFeO_3$ has a very high magnetic ordering temperature in common with other multiferroic materials as $Sr_{1-x}Ba_xMnO_3$[13], $BiFeO_3$ and $PbNiO_3$ [21]. We thus can classify $ScFeO_3$ as a type-I multiferroic, in which both ferroelectric and magnetic order exist albeit are expected to be weakly coupled.

Here we study, by means of first-principles calculations, the electronic, magnetic, and ferroelectric properties of $ScFeO_3$. Our theoretical estimate of the Néel temperature is 635 K in good agreement with the experimental observations [14]. Next we find a large ferroelectric polarization of $\sim 105\,\mu C/cm^2$ and examine its dependence on

TABLE I. Crystallographic parameters for the rhombohedral $R3c$ structure of $ScFeO_3$ obtained from PBE and PBE+U calculations. The lattice parameters are fixed to the experimental values: $a = b = 5.197$ Å, $c = 13.936$ Å, $\alpha = \beta = 90°$, $\gamma = 120°$ reported in Ref. 14.

		PBE			PBE+U = 3 eV			PBE+U = 6 eV			Experiment (Ref. 14)		
Atom	Wyck. Site	x	y	z	x	y	z	x	y	z	x	y	z
Sc	6a	0	0	0	0	0	0	0	0	0	0	0	0
Fe	6a	2/3	1/3	0.122	2/3	1/3	0.122	2/3	1/3	0.123	2/3	1/3	0.123
O	18b	0.353	-0.022	0.061	0.352	-0.023	0.060	0.353	-0.023	0.058	0.349	-0.022	0.061

the magnetic order. We find evidence of strong magnetoelectric coupling between the local Fe magnetization and the electronic contribution to the total electric polarization, which suggests that the amplitude rather than the direction of the magnetization in collinear magnets may be important in other type-I multiferroics.

II. CALCULATION DETAILS

We perform spin-polarized density functional calculations within the Perdew-Burke-Ernzerhof approximation (PBE) [22] and the PBE+U method [23] as implemented in the Vienna *Ab initio* Simulation Package (VASP) [24] with the projector augmented wave (PAW) method [25] to treat the core and valence electrons using the following electronic configurations $3p^6 4s^2 3d^1$ (Sc), $4s^2 3d^6$ (Fe), $2s^2 2p^4$ (O). A kinetic energy cutoff energy of 400 eV is used to expand the wave functions and a Γ centered 8×8×4 k-point mesh combined with the tetrahedron and Gaussian methods is used for Brillouin zone integrations. The ions are relaxed toward equilibrium until the Hellmann-Feynman forces are less than 1 meV Å^{-1} whereas the cell parameters are fixed to the experimental values [14].

It is well known that the PBE often underestimates the size of the band gap in systems with strongly localized d orbitals, therefore we also calculated the structural and electronic properties within the rotationally invariant PBE+U method [23] which requires two parameters, the Hubbard parameter U and the exchange interaction J_H. In this work, we fix the value of the Hund's exchange energy to $J_H = 0.9$ eV, as proposed for $BiFeO_3$ [26, 27] and vary the magnitude of the Hubbard parameter U between 3 and 6 eV for the Fe 3d-states. Note that the standard spin-polarized PBE corresponds to $U = J_H = 0$ eV. The electric polarization is calculated using the Berry's phase method [28] with 6 k-points for each string along the c direction.

Classical Monte Carlo (MC) simulation, with 20×20×20 supercells and 10^7 MC steps, is used to evaluate the Néel temperature.

III. RESULTS AND DISCUSSION

A. Structure

In Table I we report the atomic positions within the $R3c$ space group and the experimental lattice parameters [14] at the PBE and PBE+U with U=3 and 6 eV levels. Results for other values of U are not shown due to the similarity in results with the case U=3 and 6 eV. The atomic coordinates are in close agreement with the experimental ones [14] and are slightly affected by the Hubbard correction. The structure exhibits $a^-a^-a^-$ tilt pattern and large displacements of the Sc atoms. In the experimental structure, the FeO_6 octahedron is distorted with three short and three long Fe–O bonds of 1.96 Å and 2.15 Å respectively, resulting in an interoctaheral O–Fe–O bond angle of 135°. In our calculation this local environment is well reproduced with PBE+U with U=3 eV. In the remainder of this paper, we report results obtained using the experimental structure without ionic relaxations owing to the small difference with the equilibrium structures obtained from DFT.

B. Electronic and Magnetic Properties

Figure 1a shows the total and projected densities-of-states, calculated within the PBE for the $R3c$ structure of $ScFeO_3$. The ground state is insulating with a band gap of 0.96 eV and exhibits G-type antiferromagnetic (AFM) order with a local magnetic moment of 3.7μ_B on the Fe atoms. The valence band is composed of Fe 3d states with t_{2g} and e_g orbital character strongly hybridized with O 2p states, consistent with a high-spin d^5 cation. The strong hybridization between the Fe 3d and O 2p valence electrons, in the energy range of -6 to 0 eV, suggests that the Fe–O bonding is highly covalent.

The size of the band gap and the local magnetic moment increase as a function of U within the PBE+U formalism; in particular for U = 3 eV we find a band gap of 1.9 eV (Figure 1b) and a local magnetic moment of 4μ_B on the Fe atoms in better agreement with the experimental property measurement data [14, 29]. The introduction of the Hubbard parameter also influences the ionicity of the Fe–O bonding. Indeed, the Fe occupied 3d states are pushed down to lower energy, indicating that the Fe–O bonding is more ionic and the electrons are more localized

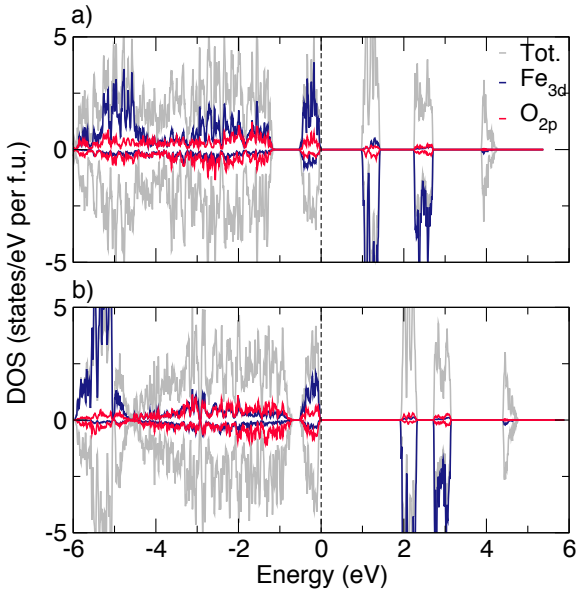

FIG. 1. (Color online) The total (gray line) and projected density of states of rhombohedral ($R3c$) $ScFeO_3$ with G-type AFM order calculated (a) with PBE and (b) PBE+U (U=3.0, J_H=0.9 eV). The zero energy is set to the top of the valence band (dashed line).

on the atomic sites, while the Fe unoccupied 3d states are pushed to higher energy.

To evaluate the magnetic ordering temperature we map the total energy of different magnetic phases on a Heisenberg model, $H = -J\sum_{ij} S_i \cdot S_j$, describing classical spins interacting only with nearest neighbors. We follow the approach of Ref. [30] and we calculate the nearest-neighbor exchange coupling J of $ScFeO_3$ from the energy difference, calculated within PBE+U with U=3 eV, between the ferromagnetic (FM) and G-type AFM order [31]. Assuming $S = 5/2$ for Fe^{3+} spins, we find an exchange interaction J = -3.3 meV, where the minus sign indicates the antiferromagnetic coupling. Using this magnetic coupling in classical Monte Carlo (MC) simulations we estimate a Néel temperature of 635 K which compares reasonably well with the experimental value of 545 K [14] given the strongly localized approximation of the adopted nearest-neighbor Heisenberg model.

C. Ferroelectricity

Figure 2a depicts the polar displacements of the Sc and O ions in the $R3c$ crystal structure. These displacements are along the [111] pseudocubic direction. This results in a spontaneous polarization along the c axis in the hexagonal setting of rhombohedral structure. The geometry-induced inversion symmetry-breaking of the $R3c$ structure with respect to the centrosymmetric $R\bar{3}c$ phase can be described by a polar mode with A_{2u} symmetry. Along the polar c axis the Sc and O ions have opposite displacements

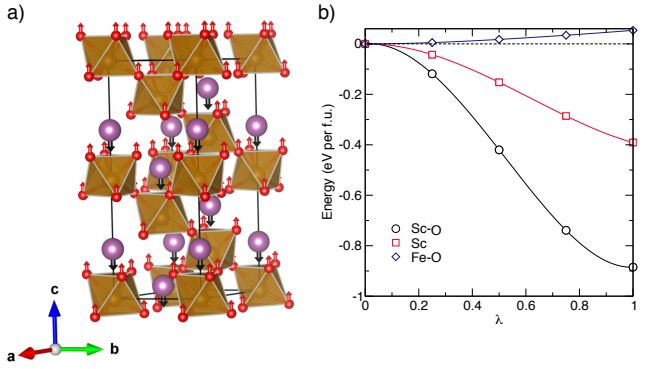

FIG. 2. (Color online) (a) Illustration of the ferroelectric displacements by the Sc and O atoms. (b) Energy gain (ΔE) as a function of the polar displacements (λ) within the PBE+U (U = 3.0 eV, J_H = 0.9 eV) with respect to the centrosymmetric $R\bar{3}c$ structure. We compare the energy of the Sc-O mode with partial modes (Sc,Fe-O) where only the listed atoms are displaced.

of -0.55 and 0.29 Å, respectively, while the Fe cations under go minor displacements and contribute weakly to the electric polarization (Fig. 2a). The situation along the non-polar a and b axes is different; the Sc and O ions exhibit antipolar displacements.

Using PBE+U = 3 eV and the G-type magnetic order, we compute the energy gain (ΔE) of the polar $R3c$ structure with respect to the centrosymmetric $R\bar{3}c$ structure as a function of λ, which is a dimensionless parameter that continuously connects the centrosymmetric $R\bar{3}c$ structure (λ=0) to the experimentally-determined polar $R3c$ structure (λ=1). Fig. 2b shows the change in energy obtained by displacing the Sc and O (Sc-O) ions participating in the A_{2u} mode versus the contributions owing to the displacements of two other subsets of ions, namely the Sc cation only and the Fe and O (Fe-O) ions. We mention in this context that the ionic positions of $R3c$ and $R\bar{3}c$ structures are interpolated by a linear relation, which is a standard procedure in the study of many multiferroic and ferroelectric materials [32–34]. We find that the $R3c$ structure is stabilized by either displacing the Sc cation or the Sc-O ions and that Fe-O distortions alone are unfavorable, leading to an increase of the total energy. Consistent with the small tolerance factor argument [14, 19] and our finding that the largest contribution to the stabilization of the polar structure comes from the polar Sc and O displacements, we conclude that the ferroelectric phase arises as a consequence of the Sc cation size. Note that the large energy-gain difference between that obtained from the Sc-O mode and the Sc mode demonstrates the decisive role played by the oxide anion.

Next, we evaluate the ferroelectric polarization using the Berry phase approach [28]. In Fig. 3 we show the total ferroelectric polarization P as a function of the Sc-O displacement mode. We find that P is weakly sensitive to the Hubbard parameter as expected by the small influence U has on the crystal structure (Table I): The magnitude of

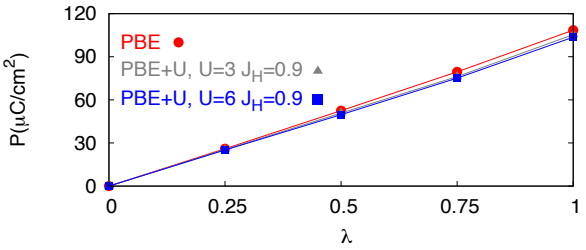

FIG. 3. (Color online) (a) The functional dependent electric polarization (P) for $ScFeO_3$ along the path connecting the paraelectric ($\lambda = 0$) and the ferroelectric structures ($\lambda = 1$).

TABLE II. Born effective charges (Z^*) for displacements along the [111]-pseudocubic direction for $ScFeO_3$ in the experimental $R3c$ crystal structure obtained from PBE and PBE+U calculations. Nominal oxidation states specified in parentheses.

	Sc (+3)	Fe (+3)	O (−2)
PBE	3.815	3.688	-2.505
PBE+U=3 eV	3.798	3.650	-2.477
PBE+U=6 eV	3.780	3.504	-2.433

the electric polarization is 108.5 μC/cm^2, 105.5 μC/cm^2, and 103.6 μC/cm^2 for $U = J_H = 0$ eV, $U = 3.0$ eV, and $U = 6.0$ eV, respectively.

In Table II we show the Born effective charges (Z^*) for the $R3c$ structure of $ScFeO_3$ as a function of the different levels of theory used in this work. In agreement with Fig. 3, we find that Z^* decreases slightly as a function of correlation U. Indeed the polarization can be written as $P \propto \sum_i Z_i ds_i$, where ds_i are the ferroelectric displacements and Z_i are the Born effective charges. Increasing U while keeping the ferroelectric displacements fixed (ds_i) we find that the effective charges get closer to the formal nominal values Sc^{3+}, Fe^{3+} and O^{2-}, which implies a smaller anomalous (electronic) contribution to P. Also, the Z^* of Sc is somewhat larger than the nominal oxidation state, indicating the importance of this ion in the the polar distortion. This is similar to $BiFeO_3$ [20] but different from $LiNbO_3$ [35], $NaNbO_3$, and $KNbO_3$ [36] where the Z^* of the A cations are much closer to the nominal values.

D. Magnetoelectric Coupling

D.I. Pure Electronic contribution to P

Although the ferroelectric polarization is mainly driven by the Sc and O atoms, we now investigate the possible existence of a magnetoelectric coupling. We use the experimental $R3c$ crystal structure to evaluate the *electronic* contribution to the ferroelectric polarization, which is a sum of the electronic and ionic contributions, by performing constrained magnetic calculations whereby the amplitude of the local Fe magnetic moment is varied

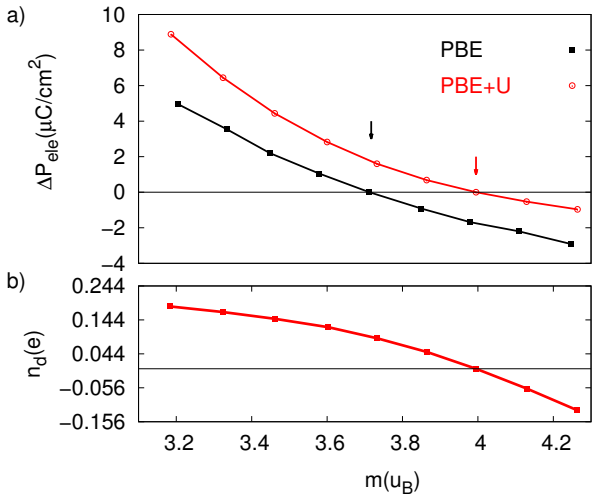

FIG. 4. (Color online) a) Change of the electronic contribution (ΔP_e) to ferroelectric polarization for $ScFeO_3$ within PBE and PBE+U (U=3.0 eV, J_H=0.9 eV) as function of the local Fe magnetization at fixed experimental ionic positions. The zero of P_{ele} is set to the value of the self-consistent calculations without constraining local Fe magnetization. b) Change of Fe charge as function of the local Fe magnetization at fixed experimental ionic positions.

(Fig. 4a). This change in the electronic polarization as a function of the local magnetic moment on the Fe site is the order of the 1 μC/cm^2 and larger than that observed in $BiFeO_3$ ($\sim 40n$C/cm^2) [10]. We find that the amplitude of the local Fe moment in the ordered G-AFM state controls the electronic P_e contribution to P.

The coupling between the electronic polarization and the local magnetic moment can be understood as a consequence of the decrease/increase in the amount of static electronic charge at the Fe site, which is donated from the oxide ions active in the inversion symmetry-breaking displacements. Indeed by inspecting the on-site density matrix of Fe ions and summing up over its eigenvalues we find that increasing the value of local magnetic moment a given amount of electronic charge is moved from Fe to O ions (see Fig. 4b). These results highlight how, once the polar displacements are active, the local spin magnetization influences the electronic contribution to the total ferroelectric polarization by changes in the d/p orbital Fe/O occupancies.

This coupling between magnetism and the electric polarization results in a 'negative' magnetoelectric coupling in $ScFeO_3$; 'negative' in the sense that the magnetic order suppresses the ferroelectric polarization. We conjecture that the same hidden magnetic effect identified in $ScFeO_3$ is likely common in other multiferroic materials like, e.g., $BiMnO_3$ [37] and $Sr_{1-x}Ba_xMnO_3$ [5]. Last, we remark here that we did not investigate the role of canting in the AFM structure (and the consequent weak ferromagnetism), but our conclusions on the local magnetization-dependent electric polarization are not expected to be sensitive to the details of the AFM state.

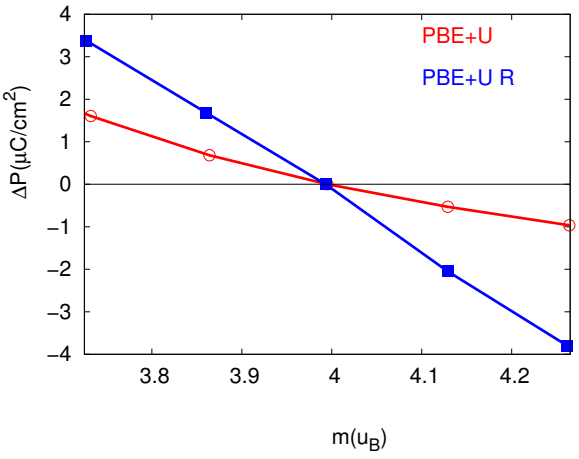

FIG. 5. (Color online) Change of the ferroelectric polarization (ΔP) for $ScFeO_3$ within PBE+U (U=3.0 eV, J_H=0.9 eV) as function of the local Fe magnetization without (PBE+U) and with ionic relaxation (PBE+U R). The zero of P is set to the value of the self-consistent calculations without constraining local Fe magnetization.

D.II. Ionic and Electronic contribution to P

As further step, in the understanding of the relation between ferroelectric polarization and onset of the magnetic ordering, we allow the ions to relax by keeping the magnetic moment at a fixed value and then we recalculate the ferroelectric polarization as sum of electronic and ionic contributions. As shown in Fig. 5, we find that the magneto-electric coupling is further enhanced by inclusion of ionic relaxations. This clearly suggests that the ferroelectric displacements are controlled by the local magnetization of Fe sites. Note that increasing the local magnetization of the Fe sites, the contribution to the ferroelectric polarization of the Sc and O ions is only slightly decreased.

IV. CONCLUSIONS

Using first-principles methods that include interaction effects (PBE, PBE+U), we investigated the electronic and magnetic structure and the origin of the ferroelectric state of $ScFeO_3$. We find that the ferroelectric instability is mainly driven by coupled polar displacements of Sc and O similar to proper ferroelectrics such as $LiNbO_3$. The electric polarization is found to be sensitive to the magnitude of the local magnetic moment on the Fe sites. We find a 'negative' magnetoelectric interaction in type-I multiferroic $ScFeO_3$, which may also be active in other multiferroic compounds.

ACKNOWLEDGMENTS

G. G. acknowledges Koji Fujita for sharing experimental data and discussions. G. G. and M. C. acknowledge financial support by European Research Council under FP7/ERC Starting Independent Research Grant "SUPERBAD" (Grant Agreement n. 240524). D.P. and J.M.R. were supported by the ARO under grant no. W911NF-15-1-0017 for financial support.

[1] N.A. Hill, J. Phys. Chem. B **104**, 6694 (2000).
[2] S.W. Cheong and M. Mostovoy, Nature Mat. **6**, 13 (2007).
[3] D. Khomskii, Physics **2**, 20 (2009).
[4] J. Wang, J.B. Neaton, H. Zheng, V. Nagarajan, S.B. Ogale, B. Liu, D. Viehland, V. Vaithyanathan, D. G. Schlom, U.V. Waghmare, N.A. Spaldin, K. M. Rabe, M. Wuttig, R. Ramesh, Science, Vol. 299 no. 5613 pp. 1719 (2003).
[5] H. Sakai, J. Fujioka, T. Fukuda, D. Okuyama, D. Hashizume, F. Kagawa, H. Nakao, Y. Murakami, T. Arima, A.Q.R. Baron, Y. Taguchi and Y. Tokura, Phys. Rev. Lett. **107**, 137601 (2011).
[6] N. Hur, S. Park, P.A. Sharma, J.S. Ahn, S. Guba, and S. W. Cheong, Nature (London) 429, 392 (2004).
[7] T. Kimura, T. Goto, H. Shintani, K. Ishizaka, T. Arima, and Y. Tokura, Nature (London) 426, 55 (2003).
[8] S. Picozzi, K. Yamauchi, B. Sanyal, I.A. Sergienko, and E. Dagotto, Phys. Rev. Lett. **99**, 227201 (2007).
[9] G. Giovannetti and J. van den Brink, Phys. Rev. Lett. **100**, 227603 (2008).
[10] S. Lee, M. T. Fernandez-Diaz, H. Kimura, Y. Noda, D. T. Adroja, S. Lee, J. Park, V. Kiryukhin, S.-W. Cheong, M. Mostovoy, and J.-G. Park, Phys. Rev. B **88**, 060103(R) (2013).
[11] A. Kadomtseva, A. Zvezdin, Y. Popov, A. Pyatakov, and G. Vorobev, JETP Lett. **79**, 571 (2004).
[12] R. D. Johnson, P. Barone, A. Bombardi, R. J. Bean, S. Picozzi, P. G. Radaelli, Y. S. Oh, S.-W. Cheong, and L. C. Chapon, Phys. Rev. Lett. **110**, 217206 (2013).
[13] G. Giovannetti, S. Kumar, C. Ortix, M. Capone and J. van den Brink, Phys. Rev. Lett. **109**, 107601 (2012).
[14] T. Kawamoto, K. Fujita, I. Yamada, T. Matoba, S. J. Kim, P. Gao, X. Pan, S. D. Findlay, C. Tassel, H. Kageyama, A. J. Studer, J. Hester, T. Irifune, H. Akamatsu and K. Tanaka, J . Am. Chem. Soc., 2014, 136 (43), pp 15291.
[15] Y. Hamasaki, T. Shimizu, S. Yasui, T. Taniyama, O. Sakata, and M. Itoh, Cryst. Growth Des. Article ASAP, (2016). DOI: 10.1021/acs.cgd.6b00770
[16] T. Zhao, A. Scholl, F. Zavaliche, K. Lee, M. Barry, A. Doran, M. P. Cruz, Y. H. Chu, C. Ederer, N. A. Spaldin, R. R. Das, D. M. Kim, S. H. Baek, C. B. Eom and R. Ramesh, Nat. Mat. 5, 823 - 829 (2006).
[17] The tolerance factor, t, can be used as a measure of the degree of distortion of a ABO_3 perovskite from ideal cubic structure. It is defined as $t = \frac{r_A + r_0}{\sqrt{2}(r_B + r_0)}$, where r_A is the radius of the A-cation, r_B is the radius of the B-cation, and r_0 is the radius of the anion.
[18] A. M. Glazer, Acta Cryst. A **31**, 756 (1975).

[19] N. A. Benedek and C. J. Fennie, J. Phys. Chem. C **117**, 13339 (2013).

[20] J.B. Neaton, C. Ederer, U.V. Waghmare, N.A. Spaldin, and K.M. Rabe, Phys. Rev. B **71**, 014113 (2005).

[21] X. F. Hao, A. Stroppa, P. Barone, A. Filippetti, C. Franchini and S. Picozzi, New Journal of Physics 16 (2014) 015030.

[22] J. P. Perdew, K. Burke, and M. Ernzerhof, Phys. Rev. Lett. **77**, 3865 (1996).

[23] A. I. Liechtenstein, V. I. Anisimov, and J. Zaanen. Phys. Rev. B **52**, R5467(R) (1995).

[24] G. Kresse and J. Furthmuller, Phys. Rev. B **54**, 11 169 (1996); G. Kresse and J. Furthmuller, Comput. Mater. Sci. **6**, 15 (1996).

[25] G. Kresse and D. Joubert, Phys. Rev. B **59**, 1758 (1999).

[26] O. E. Gonzalez-Vazquez, J. Iniguez, Phys Rev. B **79**, 064102 (2009).

[27] A.O. Shorikov, A.V. Lukoyanov, V.I. Anisimov, S.Y. Savrasov: arXiv:1503.00470v2 .

[28] R.D. King-Smith *et. al.*, Phys. Rev. B **47**, 1651 (1993); D. Vanderbilt *et. al.*, Phys. Rev. B **48**, 4442 (1994).

[29] Koji Fujita, private communication.

[30] N. Lampis, C. Franchini, G. Satta, A. Geddo-Lehmann, and S. Massidda, Phys. Rev. B **69**, 064412 (2004).

[31] The total energy of the FM-type and G-type can be written as:
$E_{FM-type}$ = E_{NM} - 6 J S_i S_j
E_{G-type} = E_{NM} + 6 J S_i S_j
in which E_{NM} represent the total energy of non-mangetic ground state (we assume S = $\frac{5}{2}$).

[32] B. B. Van Aken, T. T.M. Palstra, A. Filippetti, N. A. Spaldin.

[33] D. Puggioni and J. M. Rondinelli, Nat. Commun. **5**, 3432 (2014).

[34] R. E. Cohen and H. Krakauer, Phys. Rev. B **42**, 6416 (1990).

[35] M. Veithen and Ph. Ghosez, Phys. Rev. B **65**, 214302 (2002).

[36] W. Zhong, R.D. King-Smith, and D. Vanderbilt, Phys. Rev. Lett. **72**, 3618 1994 .

[37] T. Kimura, S. Kawamoto, I. Yamada, M. Azuma, M. Takano, and Y. Tokura, Phys. Rev. B **67**, 180401(R) (2003).